Damage-Mitigating Control of a Reusable Rocket Engine: Part II—Formulation of an Optimal Policy

Xiaowen Dai

Asok Ray
Fellow ASME

Mechanical Engineering Department,
The Pennsylvania State University,
University Park, PA 16802

This sequence of papers in two parts investigates the feasibility of damage-mitigating control of a reusable rocket engine similar to the Space Shuttle Main Engine (SSME) where the objective is to increase structural durability without any significant loss of performance. To this effect, a fatigue damage model of the turbine blades has been reported in earlier publications, and a creep damage model of the main thrust chamber coolant channel has been formulated and tested in the first part. This paper, which is the second part, synthesizes an optimal policy for open loop control of up-thrust transients of the rocket engine. Optimization is based on the integrated model of the plant, structural and damage dynamics under the constraints of fatigue and creep damage in the critical components. The results are presented to demonstrate the potential of life extension of reusable rocket engines via damage mitigating control. The concept of damage mitigation, as presented in this paper, is not restricted to control of rocket engines. It can be applied to any system where structural durability is an important issue.

Introduction

The concept and configuration of damage-mitigating control in complex dynamic systems have been introduced in recent papers by Lorenzo and Merrill (1991) and Ray et al. (1994a, 1994b) where the objective is to achieve high performance without overstraining the mechanical structures. The major benefit of damage-mitigating control is extension of service life of critical plant components accompanied by enhanced safety, operational reliability, maintainability, and availability. The motivation of damage-mitigating control in reusable rocket engines has been presented in the first part (Dai and Ray, 1996) of this sequence of papers in two parts, which investigates the feasibility of damage mitigating control of a reusable rocket engine similar to the Space Shuttle Main Engine (SSME). The critical components of the SSME, which potentially limit its functional life, have been identified as:

- Blades of the fuel turbine;
- Blades of the oxidizer turbine;
- Coolant channel ligament in the main thrust chamber.

The major tasks in the synthesis of a damage-mitigating control system (Ray et al., 1994b) for a reusable rocket engine are: (i) formulation of structural and damage models of the critical plant components; (ii) synthesis of an open-loop (feedforward) control policy to maneuver the thermo-fluid dynamics of the rocket engine along a nominal trajectory; and (iii) synthesis of an on-line closed loop (feedback) control policy to compensate for deviations from the nominal trajectory due to disturbances and uncertainties as well as to make intelligent decisions for plant operation and maintenance. The creep damage model of the coolant channel ligament, developed and verified in the first part (Dai and Ray, 1996), is combined with the continuous-time fatigue damage model of the turbine blades reported by Ray and Wu (1994a, 1994b). This integrated damage model of the three critical components is concatenated with the plant dynamic model, and is specifically suited for synthesis of an optimal control policy where the damage rate and accumulation are constrained and/or embedded within the cost functional. The interactions between the plant model, structural model and damage model are briefly discussed in the first part, and the details are given in Ray et al. (1994a) and Ray and Wu (1994a). This paper focuses on the second task of open loop control synthesis which is essential for start-up and up-thrust transients (i.e., transition to full flow/full thrust operations) of a rocket engine (Sutton, 1992). The third task of closed-loop control is a subject of current research and is not addressed here.

This paper, which is the second part in the sequence of two papers, is organized as follows. The operating principles of the rocket engine under consideration and a finite-dimensional model of the thermo-fluid dynamics are presented from the perspectives of decision and control, followed by brief descriptions of the structural and damage models of the fuel and oxidizer turbine blades. Then, an optimal policy is synthesized for open loop control of the rocket engine under specified constraints of damage rate and damage accumulation, and the results of optimization studies for up-thrust transients are presented. Finally, this two-part paper is concluded with recommendations for possible applications of this damage mitigation concept to a variety of processes where structural durability is an important issue.

System Description and Plant Dynamic Model

The plant under control is a reusable rocket engine similar to the Space Shuttle Main Engine (SSME). Fig. 1 shows a functional diagram for operations and control of the rocket engine. The propellants, namely, liquid hydrogen fuel and liquid oxygen, are individually pressurized by separate closed cycle turbopumps. Pressurized cryogenic fuel and oxygen are pumped into two high-pressure preburners which feed the respective turbines with fuel-rich hot gas. The fuel and oxidizer turbopump speeds and hence the propellant flow into the main thrust are controlled by the respective preburner. The exhaust from each turbine is injected into the main combustion chamber where it burns with the oxidizer to make the most efficient use of the energy. The oxygen flow into each of the two preburners are independently controlled by the respective servo-valves while the valve position for oxygen flow into the main thrust chamber is held in a fixed position to derive the maximum possible power from

Contributed by the Dynamic Systems and Control Division for publication in the JOURNAL OF DYNAMIC SYSTEMS, MEASUREMENT, AND CONTROL. Manuscript received by the DSCD March 15, 1994; revised manuscript received June 28, 1994. Associate Technical Editor: J. L. Stein.

the engine. The plant outputs of interest are O_2/H_2 mixture ratio and main thrust chamber pressure which are closely related to the rocket engine performance in terms of specific impulse, thrust-to-weight ratio, and combustion temperature.

A thermo-fluid-dynamic model of the plant (i.e., the rocket engine) has been formulated to satisfy the following two criteria: (i) sufficient accuracy for plant performance analysis, damage prediction, and control systems synthesis; and (ii) mathematical and computational tractability of the governing equations to generate feasible solutions for integrated systems optimization. Standard lumped parameter methods have been used to approximate the partial differential equations describing mass, momentum, and energy conservation by a set of first-order differential equations. The plant model is constructed by causal interconnection of the primary subsystem models such as main thrust chamber, preburners, turbopumps, valves, fuel and oxidizer supply header, and fixed nozzle regeneration cooling (Ray and Dai, 1995). In this model, the plant state vector consists of twenty state variables, two control inputs, and two measured variables as listed below:

State Variables:

Fuel Turbopump shaft speed	Oxidizer Turbopump shaft speed
Main thrust chamber hot-gas pressure	Main thrust chamber hot-gas density
Fuel preburner oxygen flow valve position	Oxidizer preburner oxygen flow valve position
Fuel preburner hot-gas pressure	Oxidizer preburner hot-gas pressure
Fuel preburner hot-gas density	Oxidizer preburner hot-gas density
Fuel flow rate into the fuel preburner	Fuel flow rate into the oxidizer preburner
Oxygen flow rate into the fuel preburner	Oxygen flow rate into the oxidizer preburner
Coolant side coolant wall temperature	Oxidizer flow rate into the main thrust chamber
Hot-gas side coolant wall temperature	Nozzle cooling tube wall temperature
Main thrust chamber coolant temperature	Nozzle coolant temperature

Control Inputs:

Fuel preburner oxidizer valve position	Oxidizer preburner oxidizer valve position

Measured Variables for Plant Control:

Main thrust chamber Pressure	(O_2/H_2) mixture ratio

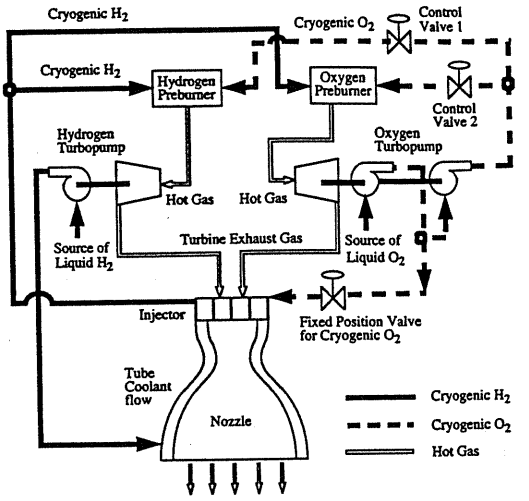

Fig. 1 Functional and operational diagram of the reusable rocket engine

Structural and Damage Model

The structural model is excited by the plant state variables to generate thermo-mechanical stresses and strains at the critical points of the engine structure which are, in turn, inputs to the damage model. For the critical components as identified earlier, the damage model is a representation of fatigue at the root of both fuel and oxidizer turbine blades, and creep and creep ratcheting of the coolant channel ligaments at the throat plane of the main thrust chamber. Since the creep damage model of the coolant channel ligament is described in the first part (Dai and Ray, 1996), only the structural and fatigue damage models of the turbine blades are briefly described here. Details are reported by Ray and Wu (1994b).

Structural Model of the Turbine Blades. The structural model in each of the fuel and oxidizer turbines calculates the cyclic mechanical stresses at the root of a typical blade which is presumed to be a critical point in this study. The blade model for each of the two turbines is represented by a three-node beam model with six degrees of freedom at each node while the first node at the root is fixed. The load on each blade model is assumed to consist of two components. The first component is due to the (time-dependent) drive torque which is derived as an output of the plant dynamic model. The second component is a dynamic term which represents the oscillatory load on the

Nomenclature

b, c = material parameter in the fatigue damage model
C = parameters in weighting matrices
D = nonlinear damage
K' = material parameter in fatigue damage model
l, m, n, p, r = dimensions of vectors and matrices
$\mathbf{M}, \mathbf{Q}, \mathbf{R}, \mathbf{S}$ = weighting matrices
n' = material parameter in the fatigue damage model
N = Number of steps in the optimization problem
$\mathbf{q}$ = output vector of the structural model
t = time
$\mathbf{u}$ = input vector of the plant model
$\mathbf{v}$ = damage state vector
W = mass flow rate
$\mathbf{W}$ = weighting vector
w = weight in the fatigue damage model
x = state vector of the plant model
y = output vector of the plant model
α = natural upper bound of the actuator position
β = damage rate constraint vector
δ = linear fatigue damage
Δt_k = (non-uniform) time interval
γ = parameter in the nonlinear fatigue damage model
Γ = damage accumulation constraint vector
ξ = incremental ratio of two consecutive time steps

Subscripts

cr = creep damage in the main thrust chamber
e = elastic part
f = final point
H_2 = fuel turbine fatigue damage
k = discrete instant of time
m = mean value of stress
N = final state in the discretized setting of the optimization problem
o = initial value
O_2 = oxidizer turbine fatigue damage
p = plastic part
r, ref = reference point
ss = steady state

blade as it passes each stator. It is the second component that causes high cycle fatigue at the root of the blade while the first component is largely responsible for the mean stress. Since both the fatigue damage and subsequent crack initiation sites are confined within a small region of the blade, a linear elastic approach is adopted for macroscopic modeling of the structural dynamics and to predict transient stresses at the point of potential failure. In this approach, the blade geometry, properties of the blade material, and plant state variables are used as inputs to the linear finite element analysis program to generate a discretized representation of the blade structure and its loading conditions. The resulting stiffness matrix, mass matrix, and force vector are used to obtain a modal solution for the displacements. In the last step, the stress-displacement relations from the finite element analysis are used to predict the stresses at the critical point(s) of the blade structure.

Continuous-Time Fatigue Damage Model of Turbine Blades. Ray and Wu (1994a) reported a methodology to model fatigue damage in the continuous-time setting as an extension of the conventional practice of cycle-based damage representation. The fatigue damage model in the continuous-time setting is first derived on the basis of linear damage accumulation following the Palmgren-Miner's rule (Bannantine et al., 1990) and then modified following the damage curve approach (Bolotin, 1989) to account for dependence of the damage rate on the current level of accumulated damage. Only the essential features of the fatigue damage model are presented in this section.

Converting the strain amplitudes into stress amplitudes from the cyclic stress-strain curve, the rates of both elastic damage δ_e and plastic damage δ_p are computed through differentiation as:

If $\sigma \geq \sigma_r$, then

$$\frac{d\delta_e}{dt} = 2\frac{d}{d\sigma}\left(\left(\frac{\sigma - \sigma_r}{2(\sigma_f' - \sigma_m)}\right)^{-1/b}\right) \times \frac{d\sigma}{dt} \tag{1a}$$

$$\frac{d\delta_p}{dt} = 2\frac{d}{d\sigma}\left(\frac{1}{\epsilon_f'}\left(\frac{\sigma - \sigma_r}{2K'}\right)^{1/n'}\left(1 - \frac{\sigma_m}{\sigma_f'}\right)^{-c/b}\right)^{-1/c} \times \frac{d\sigma}{dt} \tag{1b}$$

otherwise,

$$\frac{d\delta_e}{dt} = 0 \text{ and } \frac{d\delta_p}{dt} = 0 \tag{1c}$$

where the current stress σ and the stress rate $d\sigma/dt$ are obtained from the structural model; σ_r is the reference stress obtained using the rainflow method (Dowling, 1983; Rychlik, 1993); $\sigma_m = (\sigma + \sigma_r)/2$ is the mean stress; and σ_f', ϵ_f', b, c, K', n' are the material parameters (Bannantine et al. 1990) under cyclic operations. The damage rate $d\delta/dt$ is obtained as the weighted average of the elastic and plastic damage rates such that

$$\frac{d\delta}{dt} = w\frac{d\delta_e}{dt} + (1 - w)\frac{d\delta_p}{dt} \tag{2}$$

where the weighting function, w, is selected as the ratio of the elastic strain amplitude and total strain amplitude. Equations (1) and (2) are then used to obtain the damage rate at any instant. Since the turbine blades are subjected to leads of varying amplitude, Eq. (1) which is based on the linear rule of damage accumulation will lead to erroneous results due to the sequence effect (Suresh, 1991). Therefore, the linear damage is modified via a nonlinear damage rule as follows:

$$D = (\delta)^{\gamma(\sigma_a, D)} \tag{3}$$

where D and δ are the current states of nonlinear and linear damage accumulation, respectively, and σ_a is the stress amplitude. It follows from a crack propagation model such as the Paris model (Paris and Erdogan, 1963) that the crack growth rate is dependent not only on the stress amplitude but also on the current crack length (Ray and Wu, 1994a). Since the characteristics of γ in Eq. (3) may strongly depend on the type of the material, availability of pertinent experimental data for the correct material is essential for damage-mitigating control. An approach to evaluate γ at selected discrete levels of stress amplitude by interpolation based on the experimental data of Swain et al. (1990) for the material AISI 4340 steel is given in (Ray and Wu, 1994b).

Optimal Control Policy

The general structure of a damage-mitigating control system is reported in recent publications by Ray et al. (1994b) and Ray and Wu (1994b). The open-loop control policy was obtained via nonlinear programming (Luenberger, 1984) by optimizing a specified cost functional of the plant dynamic performance without violating pre-assigned constraints on the damage rate and damage accumulation. In this research, a general purpose nonlinear programming software NPSOL (Gill et al., 1991) has been adopted for solving this open-loop optimal control problem.

A general structure of the plant and damage dynamics, as discussed in the first part (Dai and Ray, 1996), is represented in the deterministic continuous-time setting as:

Plant dynamics:

$$\dot{\mathbf{x}} \equiv \frac{d\mathbf{x}}{dt} = \mathbf{f}(\mathbf{x}(t), \mathbf{u}(t)); \quad \mathbf{x}(t_o) = \mathbf{x}_o \tag{4}$$

Plant outputs:

$$\mathbf{y}(t) = \mathbf{g}(\mathbf{x}(t), \mathbf{u}(t)) \tag{5}$$

Structural outputs:

$$\mathbf{q}(t) = \xi(\mathbf{x}(t), \mathbf{u}(t)) \tag{6}$$

Damage dynamics:

$$\dot{\mathbf{v}} \equiv \frac{d\mathbf{v}}{dt} = \mathbf{h}(\mathbf{v}(t), \mathbf{q}(t)); \quad \mathbf{v}(t_o) = \mathbf{v}_o; \quad \mathbf{h} \geq 0 \ \forall t \tag{7}$$

where $\mathbf{x} \in \Re^n$ is the plant state vector; $\mathbf{y} \in \Re^l$ is the plant output vector, $\mathbf{u} \in \Re^m$ is the control input vector; $\mathbf{q} \in \Re^p$ is the structural model output vector; $\mathbf{v} \in \Re^r$ is the damage state vector. The nonlinear differential Eqs. (4) and (7) are assumed to satisfy the local Lipschitz condition (Vidyasagar, 1992) within the domain of the plant operating range. The state-variable representation of the damage model in Eq. (7) allows the instantaneous damage rate $\dot{v}(t)$ to be dependent on the current state of accumulated damage $v(t)$. The physical interpretation of this dependence is that a given test specimen or a plant component, under identical stress-strain hysteresis, should have different damage rates for different initial damage. The vector differential Eqs. (4) and (7) become stochastic if the randomness of plant and material parameters is included in the models, or if the plant is excited by discrete events occurring at random instants of time (Sobczyk and Spencer, 1992). The stochastic aspect of damage-mitigating control is a subject of future research, and is not addressed in this paper.

Problem Formulation. The problem is to generate, for upthrust transient operations of the rocket engine, an optimal control sequence that will not only make a trade-off between the performance and damage but also strike a balance between potentially conflicting requirements of damage mitigation at the individual critical points. The task to be accomplished is to identify an optimal control sequence $\{\mathbf{u}_k\}$ such that the plant is steered from the known plant state $\mathbf{x}_o$ and the damage state

$\mathbf{v}_o$ at the initial time, t_o, to the specified steady state $\mathbf{x}_{ss}$ and the corresponding control effort $\mathbf{u}_{ss}$ at the final time t_f. The quadratic cost functional is chosen to be the square of the weighted l_2-norm of the plant states, selected plant output, control efforts, final state errors and time derivatives of the damage states. The steps for generating the optimal control policy are as follows: Minimize the cost functional:

$$J(\tilde{\mathbf{u}}_k) = \tilde{\mathbf{x}}_N^{\mathrm{T}}\mathbf{M}\tilde{\mathbf{x}}_N + \sum_{k=o}^{N-1} [\tilde{\mathbf{x}}_k^{\mathrm{T}}\mathbf{Q}\tilde{\mathbf{x}}_k + \tilde{\mathbf{y}}_k^{\mathrm{T}}\mathbf{S}\tilde{\mathbf{y}}_k + \tilde{\mathbf{u}}_k^{\mathrm{T}}\mathbf{R}\tilde{\mathbf{u}}_k + \mathbf{W}^{\mathrm{T}}\dot{\mathbf{v}}_k]\Delta t_k \quad (8)$$

under the following equality constraints representing the plant, structural and damage characteristics:

$$\mathbf{x}_{k+1} = \mathbf{x}_k + \int_{t_k}^{t_{k+1}} \mathbf{f}(\mathbf{x}(t), \mathbf{u}(t))dt; \quad \mathbf{x}_k = \mathbf{x}(t_k) \quad (9)$$

$$\mathbf{y}_k = \mathbf{g}(x_k, \mathbf{u}_k); \quad \mathbf{u}_k = \mathbf{u}(t_k) \quad (10)$$

$$\mathbf{v}_{k+1} = \mathbf{v}_k + \int_{t_k}^{t_{k+1}} \mathbf{h}(\mathbf{v}(t), \mathbf{q}(t))dt; \quad \mathbf{v}_k = \mathbf{v}(t_k) \quad (11)$$

$$\mathbf{q}_k = \mathbf{q}(\mathbf{x}_k, \mathbf{u}_k) \quad (12)$$

and the following inequality constraints representing the natural bounds of actuator saturation and design specifications of bounds on damage rate and accumulation:

$$0 \le \tilde{\mathbf{u}}_k < \tilde{\alpha}_k \quad (13)$$

$$0 \le \mathbf{h}(\mathbf{v}_k, \mathbf{q}_k) < \beta_k \quad (14)$$

$$(\mathbf{v}_N - \mathbf{v}_o) < \Gamma \quad (15)$$

where N is the total number of discretized steps which represent the period from the initial time, t_o, to the final time t_f; Δt_k is the (possibly) non-uniform time interval, $\Delta t_k = t_{k+1} - t_k$, for $k = 1, 2,$ to N; $\{\mathbf{x}_k\} \in \Re^{n\times N}$ is the sequence of N plant state vectors; $\{\mathbf{y}_k\} \in \Re^{l\times N}$ is the sequence of N plant output vectors; $\{\mathbf{u}_k\} \in \Re^{m\times N}$ is the sequence of N control input vectors; $\{\mathbf{q}_k\} \in \Re^{p\times N}$ is the sequence of N structural output vectors; $\{\mathbf{v}_k\} \in \Re^{r\times N}$ is the sequence of N damage state vectors; $\{\tilde{\alpha}_k\} \in \Re^{m\times N}$ is the sequence of N normalized natural bound vectors of the actuator (valve) positions; $\{\beta_k\} \in \Re^{r\times N}$ is the sequence of N (possibly) time-dependent tolerances for the damage rate vectors; $\Gamma \in \Re^r$ is the specified tolerances for the damage accumulation vector; $\{\tilde{\mathbf{x}}_k\} \in \Re^{n\times N}$ is the sequence of N normalized deviations of plant state vectors; $\{\tilde{\mathbf{y}}_k\} \in \Re^{l\times N}$ is the sequence of N normalized deviation of plant output vectors; $\{\tilde{\mathbf{u}}_k\} \in \Re^{m\times N}$ is the sequence of N normalized deviations of the control input vectors; $\{\tilde{\mathbf{v}}_k\} \in \Re^{r\times N}$ is the sequence of N damage rate state vectors. The definitions of the above normalized vectors for $k = 1, 2,$ to N are given as:

$$\tilde{x}_k^i = (x_k^i - x_{ss}^i)/x_{ss}^i, \; i = 1, 2, \ldots, n; \quad \mathbf{x}_k = [x_k^1, x_k^2, \ldots, x_k^n] \quad (16a)$$

$$\tilde{y}_k^i = (y_k^i - y_{ss}^i)/y_{ss}^i, \; i = 1, 2, \ldots, l; \quad \mathbf{y}_k = [y_k^1, y_k^2, \ldots, y_k^l] \quad (16b)$$

$$\tilde{u}_k^i = (u_k^i - u_{ss}^i)/u_{ss}^i, \; i = 1, 2, \ldots, m; \quad \mathbf{u}_k = [u_k^1, u_k^2, \ldots, u_k^m] \quad (16c)$$

The weighting matrices $\mathbf{M}$, $\mathbf{Q}$, $\mathbf{R}$, and $\mathbf{S}$ in the cost functional in Eq. (8) are symmetric positive semi-definite and have compatible dimensions; and the weighting vector $\mathbf{W}$ has non-negative elements. The damage in the critical components can be reduced by adjusting the weighting vector $\mathbf{W}$ and/or by restricting the damage rate and accumulation via the constraints in Eqs. (14) and (15). Therefore, the last term on the right hand side of Eq. (8) is optional as it minimizes the accumulated damage in the critical components in addition to the application of the constraints on the damage rate and accumulation. The purpose of including the plant output vector deviation $\tilde{\mathbf{y}}(t)$ in the cost functional is to inhibit any large deviation of the specific output variable from its desired value. In this specific case, the output variable of interest is the oxygen/fuel O_2/H_2 mixture ratio because the rocket engine performance and propellant utilization are very sensitive to the mixture ratio which should be maintained at the desired value of 6.02 during the transients. Therefore, $\mathbf{S}$ is a (1×1) matrix in this case because only one output variable has been selected.

To realize physical significance of the weighting parameters, the matrices $\mathbf{M}$, $\mathbf{Q}$, and $\mathbf{R}$ in Eq. (8) are chosen to be diagonal and constant. Furthermore, these matrices are normalized relative to the non-dimensional vectors $\tilde{\mathbf{x}}_k$, and $\tilde{\mathbf{u}}_k$ in the cost functional J of Eq. (8), and the weights in $\mathbf{M}$, $\mathbf{Q}$, $\mathbf{R}$, $\mathbf{S}$, and $\mathbf{W}$, as chosen in this study, are delineated below.

$$\mathbf{Q}_{n\times n} = \frac{1}{(n + C_{33} - 1)} \begin{bmatrix} 1 & & & & \\ & 1 & & & 0 \\ & & C_{33} & & \\ & & 0 & \ddots & \\ & & & & 1 \end{bmatrix}$$

$$\text{such that} \quad tr(\mathbf{Q}) = 1 \quad (17a)$$

$$\mathbf{S}_{1\times 1} = C_{SQ} \quad (17b)$$

$$\mathbf{R}_{m\times m} = \frac{C_{RQ}}{m} \begin{bmatrix} 1 & 0 \\ 0 & 1 \end{bmatrix}_{m\times m} \quad \text{such that} \quad tr(\mathbf{R}) = C_{RQ} \quad (17c)$$

$$\mathbf{M}_{n\times n} = C_{MQ} \times \mathbf{Q}_{n\times n} \quad \text{such that} \quad tr(\mathbf{M}) = C_{MQ} \quad (17d)$$

$$\mathbf{W}_{r\times 1} = \mathbf{O}_{r\times 1} \quad (17e)$$

where the scalar constants, C_{MQ}, C_{SQ} and C_{RQ} in the weighting matrices $\mathbf{Q}$, $\mathbf{S}$, $\mathbf{R}$, and $\mathbf{M}$ represent their respective importance relative to the weighting matrix $\mathbf{Q}$; and the elements of $\mathbf{W}$ are set identically to 0 implying that the damage rate is not penalized in the cost functional. This approach reduces the variety of choices for weighting matrices. The diagonal elements of the weighting matrix $\mathbf{Q}$ could be different because they correspond to the respective plant state variables which are not equally important in terms of the plant performance. In the plant model, the main thrust chamber pressure which is the third state variable is more heavily weighted than others because it is strongly related to the engine performance.

For solving the nonlinear optimization problem, the scalar weighting parameters in matrices $\mathbf{M}$, $\mathbf{Q}$, $\mathbf{S}$, and $\mathbf{R}$ are chosen as $C_{33} = 30$; $C_{SQ} = 2.175$; $C_{RQ} = 0.002$, and $C_{MQ} = 0$. The optimal decision variables to be identified are the control input sequence $\{u_k\}$ having the dimension of $m \times N$ for $k = 0, 1, \ldots, N - 1$. To capture the fast dynamics at an early stage of transients, time steps Δt_k are chosen to be non-uniform as follows:

$$\Delta t_k = \xi \Delta t_{k-1}, \quad k = 1, 2, \ldots, N \quad (18)$$

where the constant $\xi > 1$ is the incremental ratio of two consecutive time steps. This setting of non-uniform time steps enhances the computational efficiency of numerical optimization process by reducing the total number steps of N (i.e., the dimension of the decision vector in the optimization problem) for the same period $(t_f - t_o)$ without any significant loss of accuracy. The fixed-step Runge-Kutta scheme has been used to numerically solve the integrals in Eqs. (2) and (4).

Results and Discussion

The purpose of these optimization studies is to examine the dynamic performance of the rocket engine while constraining the rate and accumulation of fatigue and creep damage in the

Table 1 The damge rate constraints $\beta(t)$ and initial damage D_o under the optimization condition 1

Optimization condition 1	Fuel turbine $\beta_{H_2}(t)/D_{o,H_2}$	Oxidizer turbine $\beta_{O_2}(t)/D_{o,O_2}$	Coolant channel ligament $\beta_{cr}(t)/D_{o,cr}$
Case 1A	Unconstrained/ 0.1	Unconstrained/ 0.1	Unconstrained/ 0.0088
Case 1B	Unconstrained/ 0.1	Unconstrained/ 0.1	1.3×10^{-3} sec^{-1}/ 0.0088
Case 1C	Unconstrained/ 0.1	Unconstrained/ 0.1	0.6×10^{-3} sec^{-1}/ 0.0088

critical components. Based on the optimal control policy, the transients of the process variables and the resulting damage in the critical components were obtained by manipulating the two oxidizer valves in Fig. 1. The rocket engine model is maneuvered from the initial equilibrium state of chamber pressure at 2700 psi and mixture ratio of 6.02 to the new equilibrium state of chamber pressure at 3000 psi and the same mixture ratio of 6.02 in 300 ms. The control commands to the two preburner oxidizer valves are updated at 37 discrete time instants (i.e., $N = 37$) in which the parameters in Eq. (18) were selected as: $\xi = 1.035$ and $\Delta t_1 = 3$ ms. The cost functional to be minimized is based on the deviations from the final equilibrium state at 3000 psi.

Optimization has been carried out under different damage rate constraints and different initial damage in the critical plant components, namely, fuel turbine blades, oxidizer turbine blades, and the coolant channel ligament in the main thrust chamber. Pertinent results presented in this section are three cases with different creep damage rate constraints in the coolant channel ligament for a given initial creep damage. The initial fatigue damage in the fuel and oxidizer turbine blades are set to $D_{o,H2} = D_{o,O2} = 0.1$ in each of these three cases, and no fatigue damage constraints are imposed. The initial damage and constrained damage rates for the turbines blades and coolant channel ligament are listed in Table 1.

Visco-elasto-plastic parameters of oxygen free high conductivity copper (Freed and Verrelli, 1988), which was used as the coolant channel ligament in earlier versions of the SSME, have been used in these optimization studies. Similar parameters for NARloy-Z, a copper-Zirconium-Silver alloy, which is currently used as the ligament material in the SSME, are reported in other publications (Dai and Ray, 1995; Ray and Dai, 1995). However, due to unavailability of the appropriate data for Inconel 718 and MAR-M-246 which are the actual turbine blade materials used in the rocket engines, the fatigue damage parameters of the turbine blades were obtained from the report of Ray and Wu (1994b), which are based on the properties of AISI 4340 steel (Swain et al., 1990). Therefore, precise conclusions regarding the blade fatigue damage cannot be made based on these optimization results until the damage parameters of the actual material are available.

The transients in Figs. 2 to 4 exhibit the dynamics of various engine variables and the damage resulting from optimization over the time period of 0 to 300 ms where the control action is updated at the thirty seven ($N = 37$) non-uniformly spaced discrete instants of time. Figure 2 shows the transients of the creep damage rate and accumulation in the coolant channel ligament corresponding to the constraints laid out in Table 1. The creep damage rate is restrained within the prescribed constraints, and the accumulated creep damage in the coolant channel ligament is monotonically decreased as the constraint is made stronger. Therefore, service life of the main thrust chamber can be extended by imposing constraints on the creep damage rate. For the same initial creep damage in the ligament, creep damage rates near the final equilibrium state are almost identical for all three cases in Table 1; and the growth rates of creep damage accumulation are not much different except during the initial transition period. The peak of the creep damage rate occurs between about 10 ms and 30 ms, which follows the dynamic response of the inputs to the creep damage model, i.e. the temperature and pressure loading on the ligament.

The transients of the fatigue damage rate and fatigue damage accumulation for the fuel turbine blades are shown in Fig. 3 under different creep damage constraints on the ligament. Since the fatigue damage rate in the turbine blades is largely determined by instantaneous values of the mean stress and stress amplitude, the accumulated fatigue damage is reduced and slowed down for the constrained cases as seen in Fig. 3. The optimization results also indicate that constraining the creep damage rate in the coolant channel ligament has a direct effect on the fatigue damage in the fuel and oxidizer turbine blades, even though no fatigue damage constraints are imposed on the turbine blades. By imposing a constraint on the creep damage rate, service life of the coolant channel is increased with a simultaneous increase in service life of the fuel turbine. The fatigue damage accumulation in the turbine blades under the creep damage constraint in the ligament (Case 1B and Case 1C) is about one-sixth of that in the unconstrained cases (Case 1A). Similar results for the oxidizer turbine, which are not presented in this paper due to space limitation, are reported in a NASA publication (Ray and Dai, 1995).

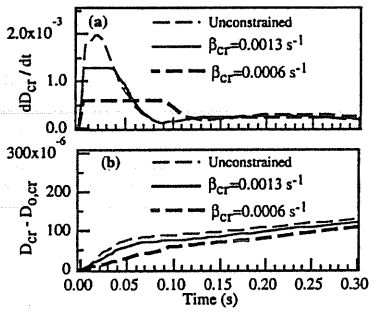

Fig. 2 Transients of creep damage of the ligament

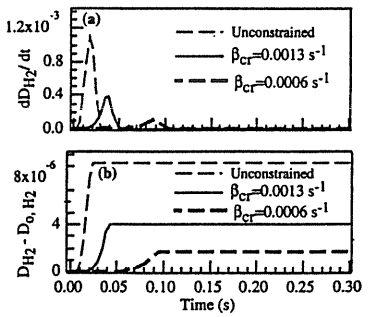

Fig. 3 Transients of fuel turbine fatigue damage

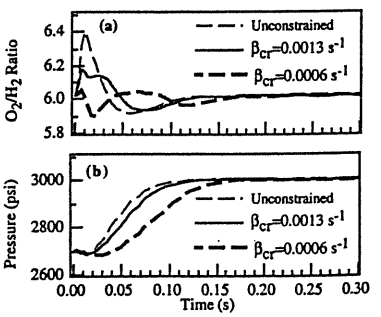

Fig. 4 Transients of plant performance

Table 2 The damage rate constraints $\beta(t)$ and initial damage D_o under optimization condition 2

Optimization condition 1	Fuel turbine $\beta_{H_2}(t)/D_{o,H_2}$	Oxidizer turbine $\beta_{O_2}(t)/D_{o,O_2}$	Coolant channel ligament $\beta_{cr}(t)/D_{o,cr}$
Case 1A	Unconstrained/ 0.1	Unconstrained/ 0.1	1.3×10^{-3} s^{-1}/ 0.0088
Case 1B	Unconstrained/ 0.1	Unconstrained/ 0.1	1.3×10^{-3} s^{-1}/ 0.189
Case 1C	Unconstrained/ 0.1	Unconstrained/ 0.1	1.3×10^{-3} s^{-1}/ 0.460

Figure 4 shows how the plant dynamic performance is influenced by different creep damage constraints in the ligament. The resulting transients of the key process variables, namely, O_2/H_2 mixture ratio and hot-gas pressure in the main thrust chamber, are shown in Fig. 4. For a given initial damage, the net excursion of the mixture ratio in Figure 4(a) is in the range of 5.9 to 6.4 for the unconstrained case, and is improved to 5.9 to 6.04 for the constrained case during these up-thrust transients of the rocket engine. This indicates that constraining the damage rate may actually improve the oscillatory behavior of the mixture ratio as seen in Fig. 4(a). However, as expected, both mixture ratio and pressure dynamics tend to become more sluggish as the damage rate constraint is made stronger.

Due to space limitation, only typical results for three cases (as listed in Table 2) are presented here for different initial creep damage under the same constraint of the creep damage rate in the coolant channel ligament. The creep damage rate and accumulation in the ligament are shown in Fig. 5 for different initial creep damage. The growth of creep damage accumulation for a larger initial damage is faster than that for a smaller initial damage under a given constraint of the creep damage rate. The rationale is that, under severe thermo-mechanical loading, structural behavior of the ligament is nonlinear due to a combination of geometric deformation and viscoplasticity. Specifically, initial conditions of the inelastic strain state vector and initial creep damage based on the current shape of the ligament are responsible for this nonlinear creep damage behavior. The above results indicate that deformed shape of the ligament is a critical factor in the creep damage model developed in the first part (Dai and Ray, 1996). Optimization studies were also conducted under different fatigue damage constraints and initial fatigue damage in the fuel and oxidizer turbine blades. These results are not presented here as their characteristics are largely similar to those reported in our previous publication (Ray et al., 1994c) in which creep damage in the ligament was not investigated.

Summary and Conclusions

The theme of the research in damage mitigating control of reusable rocket engines, as presented in this two-part paper, is summarized below:

- High performance of rocket engines can be achieved without overstraining the mechanical structures such that the functional life of critical components are increased.
- On-line damage prediction and damage mitigation, based on the available sensory and operational information, will allow reusable rocket engines to be inexpensively maintained, and safely and efficiently manipulated under diverse operating conditions.

The feasibility of applying this control concept to a reusable rocket engine similar to the Space Shuttle Main Engine (SSME) has been investigated in view of fatigue and creep damage in three critical components, namely, the fuel turbine, the oxidizer turbine, and the main thrust chamber. A creep damage model of the coolant channel ligament in the main thrust chamber has been formulated. The results predicted by this model are in agreement with those obtained from finite element analyses and experimental observations. Based on the fatigue damage model, reported earlier, and this creep damage model, an optimal policy has been synthesized for open-loop control of up-thrust transients under the damage constraints in the above three critical components of the rocket engine.

The results of optimization studies demonstrate the interactive nature of fatigue damage in the fuel and oxidizer turbine blades, and creep damage in the coolant channel ligament of the main thrust chamber. The damage accumulation in both coolant channel ligament and turbine blades are shown to be significantly influenced by their respective constraints and initial damage. It is observed that the initial damage in the critical components may have a significant impact on the service life extension of rocket engines. Therefore, in the synthesis of a control policy, both the constraints and performance cost functional need to be selected based on the knowledge of the initial damage in the critical components.

Up-thrust transients of the rocket engine from an initial state of the chamber pressure at 2700 psi to the final state at 3000 psi have been simulated for a very brief period of 300 ms. Complete operations of a reusable rocket engine over its life include many such transients, and the steady-state operation in a single flight may last for several hundreds of seconds. Although both fatigue and creep damage rates during the steady state are smaller than those during transient operations, the total damage accumulation during steady state operations may not be insignificant. Therefore, during one flight of a reusable rocket engine, the cumulative effects of both transient and steady state operations need to be considered for estimation of total damage accumulation.

The optimization studies presented in this paper only consider a single point in each of the three critical components. Simultaneous control of damage at several other critical points in the rocket engine might be necessary for damage mitigation and life extension. However, this will make the optimization problem more complex as the dimension of the damage vector becomes large compared to the three-dimensional damage vector in the present study.

Although a significant amount of research has been conducted in each of the individual areas of Controls and Materials, integration of these disciplines for optimal design of complex thermo-mechanical systems has not apparently received much attention. As the science and technology of materials continue to evolve, systems analysis and design methodologies must have the capability of easily incorporating an appropriate representation of material properties, structural behavior, and thermo-fluid dynamics in the control synthesis procedure. The challenge here is to characterize the thermo-mechanical behavior of structural materials for life prediction in conjunction with dynamic performance analysis of thermo-fluid processes, and then utilize this information in a mathematically and computationally tractable form for synthesizing decision and control algorithms. There-

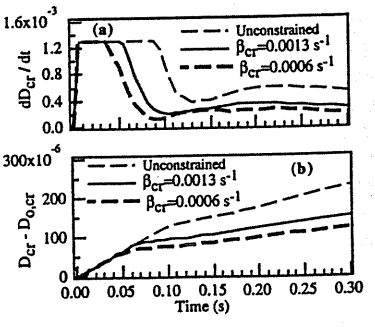

Fig. 5 Transients of creep damage of the ligament

fore, this evolutionary research in damage mitigating control requires integration of the disciplines of Controls, Thermo-Fluids, Structures, and Materials (Ray et al., 1994d).

The concept of damage mitigation, as presented in this paper, is not restricted to rocket engines. It can be applied to any system where structural durability is an important issue. Besides rocket engines, applications of damage-mitigating control include a wide spectrum of engineering applications such as fossil and nuclear plants for electric power generation, rotating and fixed wing aircraft, automotive and truck engine/transmission systems, and large rolling mills. In each of these systems, damage-mitigating control can enhance safety and productivity accompanied by reduced life cycle cost. For example, the availability of power plants often suffers from premature failures of steam generator tubes (due to corrosion-fatigue and creep), main steam and reheat steam pipelines (due to creep and fatigue), condenser tubes (due to stress corrosion cracking and flow-induced vibration) and low pressure turbine blades (due to stress corrosion, erosion, and fatigue). A continuous-time damage model will allow timely warnings of these failures, and the resulting decision and control actions will not only avoid an early shutdown but also improve maintainability. A more complex application of the damage mitigation concept is start-up and scheduled shutdown of power plants, and take-off and landing of commercial aircraft, in which the damage information can be utilized for real-time plant control either in the fully automated mode or with human operator(s) in the loop. Another example is the control of automotive engine and transmission systems to reduce stresses in the drive-train components without compromising driving performance and comfort. The result will be a combination of extended life and reduced drive-train mass with associated savings in the fuel consumption.

Acknowledgments

The authors acknowledge benefits of discussion with Professor Marc Carpino of Penn State University and Mr. Carl F. Lorenzo of NASA Lewis Research Center.

The research work reported in this paper has been supported in part by:

NASA Lewis Research Center under Grant No. NAG 3-1240.

NASA Lewis Research Center under Grant No. NAG 3-1673.

National Science Foundation under Research Grant No. ECS-9216386.

National Science Foundation under Research Grant No. DMI-9424587.

Office of Naval Research under Grant No. N00014-90-J-1513.

Electric Power Research Institute under Contract No. EPRI RP8030-5.

National Science Foundation under Research Equipment Grant No. MSS-9112609.

References

Bannantine, J. A., Comer, J. J., and Handrock, J. L., 1990, *Fundamentals of Metal Fatigue Analysis,* Prentice Hall, NJ.

Bolotin, V. V., 1989, *Prediction of Service Life for Machines and Structures,* ASME Press.

Dai, X., and Ray, A., 1995, "Life Prediction of the Thrust Chamber Wall of a Reusable Rocket Engine," *AIAA Journal of Propulsion and Power,* in press.

Dai, X., and Ray, A., 1996, "Damage Mitigating Control of a Reusable Rocket Engine: Part I—Life Prediction of the Combustion Chamber Coolant Wall," ASME JOURNAL OF DYNAMIC SYSTEMS, MEASUREMENT, AND CONTROL. Published in this issue pp. 401–408.

Dowling, N. E., 1983, "Fatigue Life Prediction for Complex Load Versus Time Histories," Journal of Engineering Materials and Technology", *Trans. ASME,* Vol. 105, pp. 206–214.

Freed, A. D., and Verrilli, M. J., 1988, "A Viscoplastic Theory Applied to Copper," NASA TM-100831.

Gill, P. E., Murray, W., Saunders, M. A., and Wright, M. H., 1991, NPSOL Version 4.06, Software Distribution Center, Stanford University, 1991, Palo Alto, CA.

Lorenzo, C. F., and Merrill, W. C., 1991, "An Intelligent Control System for Rocket Engines: Need, Vision, and Issues," *Control Systems Magazine,* Vol. 12, No. 1. Jan., pp. 42–46.

Luenberger, D. G., 1984, *Linear and Nonlinear Programming,* 2nd edition, Reading, Mass., Addison-Wesley, Menlo Park, CA.

Paris, P. C., and Erdogan, F., 1963, "A Critical Analysis of Crack Propagation Laws," ASME *Journal of Basic Engineering,* Vol. D85, pp. 528–534.

Ray, A., and Wu, M-K., 1994a, "Fatigue Damage Control of Mechanical Systems," *SMART Materials and Structures,* Vol. 3, No. 1, March 1994, pp. 47–58.

Ray, A., and Wu, M-K., 1994b, *Damage-Mitigating Control of Space Propulsion Systems for Structural Durability and High Performance,* NASA Lewis Research Center Contractor Report 194470, March.

Ray, A., Wu, M-K., Carpino, M., and Lorenzo, C. F., 1994a, "Damage-Mitigating Control of Mechanical Systems: Part I - Conceptual Development and Model Formulation," ASME JOURNAL OF DYNAMIC SYSTEMS, MEASUREMENT, AND CONTROL, Vol. 116, No. 3, pp. 437–447.

Ray, A., Wu, M-K., Carpino, M., and Lorenzo, C. F., 1994b, "Damage-Mitigating Control of Mechanical Systems: Part II - Formulation of an Optimal Policy and Simulation," ASME JOURNAL OF DYNAMIC SYSTEMS, MEASUREMENT, AND CONTROL, Vol. 116, No. 3, pp. 448–455.

Ray, A., Dai, X., Wu, M-K., Carpino, M., and Lorenzo, C. F., 1994c, "Damage-Mitigating Control of a Reusable Rocket Engine," *AIAA Journal of Propulsion and Power,* Vol. 10, No. 2, March-April, pp. 225–233.

Ray, A., Dai, X., Wu, M-K., Carpino, M., and Lorenzo, C. F., 1994d, "Damage-Mitigating Control - An Interdisciplinary Thrust between Controls and Material Science," American Control Conference, Baltimore, MD, June-July, pp. 3449–3453.

Ray, A., and Dai, X., 1995, "Damage-Mitigating Control of a Reusable Rocket Engine for High Performance and Extended Life," NASA Contractor Report 4640, NASA Lewis Research Center.

Rychlik, I., 1993, "Note on Cycle Counts in Irregular Loads," *Fatigue & Fracture of Engineering Materials & Structures,* Vol. 16, No. 4, pp. 377–390.

Sobczyk, K., and Spencer, B. F., Jr., 1992, *Random Fatigue: Data to Theory,* Academic Press, Boston, MA.

Suresh, S., 1991, *Fatigue of Materials,* Cambridge University Press, Cambridge, U.K.

Sutton, G. P., 1992, *Rocket Propulsion Elements, An Introduction to the Engineering of Rockets.* Wiley Interscience, New York.

Swain, M. H., Everett, R. A., Newman, J. C., Jr., Phillips, E. P., 1990, "The Growth of Short Cracks in 4340 Steel and Aluminum-Lithium 2090," AGARD Report, No. 767, pp. 7.1–7.30.

Vidyasagar, M., 1992, *Nonlinear Systems Analysis,* 2nd ed., Prentice Hall, Englewood Cliffs, NJ.